Annals of Nuclear Energy 179 (2022) 109421

Contents lists available at ScienceDirect

Annals of Nuclear Energy

journal homepage: www.elsevier.com/locate/anucene

The feasibility study of the Sub-criticalization of the Holos small modular reactor driven by an electron accelerator

Mohammad Mahdi Firoozabadi [a,*], Sareh Arhami [a], Zohreh Golamzadeh [b], Mahdi Zangian [c]

[a] Department of Physics, Faculty of Sciences, University of Birjand, University Blvd., Birjand, Southern Khorasan, Iran, P.O.B: 9717434765
[b] Reactor and Nuclear Safety Research School, Nuclear Science and Technology Research Institute (NSTRI), Tehran, Iran, P.O.B: 14399-51113
[c] Nuclear Engineering Department of Shahid Beheshti University, Evin, Tehran, Iran, P.O.B: 1985963113

ARTICLE INFO

Keywords:
Holos portable reactor
Accelerator driven sub-critical reactor
Small modular reactor
Electron accelerator
MCNPX2.6 code

ABSTRACT

Small modular reactors (SMRs) and accelerator-driven subcritical reactors (ADSs) have many potentials, which have attracted the attention of many researchers. The present study proposes the sub-criticalization of a small portable reactor to increase its safety. The operation of the Holos mobile power generator is examined at the subcritical level to produce cost-effective power. The UO2-fueled Holos subcritical core is modelled by the MCNPX2.6 code. The external photoneutron source was considered with a 100 MeV, 1 mA electron accelerator. The Holos simulated core is discussed in the subcritical level to evaluate the neutronic performance and safety parameters. Power distributions were compared inside the Holos simulated core in critical and subcritical levels. The carried-out calculations show that in addition to the subcritical level operation, negative reactivity coefficient in the Holos subcritical core ensures the core inherent safety. Results show that the neutron and photon flux magnitudes within the Holos core in the subcritical level are greater than the critical state.

1. Introduction

HolosGen has developed mobile scalable integral nuclear generators with a simplified and innovative design optimized to produce economical, distributable, pollutant-free and, most importantly, safe electricity. The Holos core is composed by coupling four modules, and the resulting paired core becomes critical. It produces an electric power of 3 MWe to 81 MWe only when Holos modules are brought together, thus forming the whole core. The mechanical branches of modules control their location and adjust the core power level. If the whole core of Holos becomes subcritical and it occurs mechanical errors, the possibility of nuclear accidents will reduce. HolosGen uses a high-efficiency heat conversion system (turbojet) in which inert helium gas circulates in a closed path, and the gas fluid transfers the core fission heat to the power conversion cycle. The Holos reactor is a type of small modular reactor (SMR). The global interest has been increased in small modular reactors because of their outstanding characteristics compared to large reactors. SMR modules are made in factories throughout the world, and they are shipped to remote areas for the installation. Due to their small size, they are suitable for generating electricity in distant cities where large scale reactors cannot operate (Magruder et al., 2018; Filippone & Jordan, 2017). These types of small and portable reactors are used for a variety of applications.

Ingersoll et al. (2014) presented that a NuScale small modular reactor could effectively pair to various desalination technologies. Their results show that these systems are suited for cogenerating electricity and clean water. This study provides a cost-effective approach to expanding global desalination capacity (Ingersoll et al., 2014).

The greatest challenge of the nuclear industry is the management of the highly radioactive nuclear waste and fissile element reserves. Research on an innovative concept of a hybrid system or an Accelerator Driven Subcritical Reactor (ADSR) has begun since 1993. These reactors are often applied to transmute long-lived radioisotopes to materials with a much shorter half-life, and they can simultaneously generate electricity. Both Thorium and Uranium oxide fuel cycles can be used in these reactors. The ADS reactor includes a high-power proton accelerator, a spallation target, and a subcritical core. The principal role of the spallation target is the production of primary neutrons, and the ADS core multiplies spallation neutrons. Two advantages of the ADS reactors are that it quickly shuts down when the accelerator switches off. It also works at the subcritical level, so they are safer than critical reactors (Nifenecker et al., 2001).

Abbreviations: SMR, Small modular reactor; ADSR, Accelerator-driven subcritical reactor; HolosGen, Holos Generator.

* Corresponding author.
E-mail address: Mfiroozabadi@birjand.ac.ir (M. Mahdi Firoozabadi).

https://doi.org/10.1016/j.anucene.2022.109421
Received 9 September 2021; Received in revised form 6 May 2022; Accepted 23 August 2022
Available online 30 August 2022
0306-4549/

In order to drive an ADSR by a proton accelerator, the proton beam energy of ~ 1 GeV is required. Above this proton energy, there is only marginal neutronics gain but below this, there is a sharp fall. However, the construction cost of a high-power proton accelerator is considered to become expensive and to a considerable extent it has an unstable beam. A comparison between the construction cost of spallation neutron sources and photoneutron sources is presented in Fig. 1. As can be seen from this figure, the construction cost of a spallation neutron source with an output of 10^{16} is almost 4 times higher than a photoneutron source with the same output. Moreover, the proton accelerators must have capability to dissipate very high heat flux without vaporizing (heat flux of the order > 1 kW/cm^3) in comparison with the electron accelerators. The optimized size of the target of the proton-based system, in terms of the volume was estimated to be 16 times larger than that of the electron-based system. Due to the smaller size of the target in the electron accelerator systems, implementation of multiple targets into the subcritical reactor system is a possibility to increase the neutron production rate. This will also help to flatten the spatial neutron flux distribution in the core. Hence, the electron-LINAC-based neutron source could be an attractive choice to improve the performance of neutron source under a restricted construction cost and engineering issues.

In this paper, the subcriticalization of a small portable reactor discusses because of the outstanding features of ADS reactors. Finally, an immediate power generation system will be designed computationally so that it supplies electricity to many near and far areas in natural situations or emergencies. In this study, the Holos small portable core is considered because of the arrangement of the Holos core and the High-efficiency heat conversion system (turbojet). One of the safe design potentials of small modular reactors is the use of an accelerator-driven subcritical design.

Many researchers of different countries have performed computational and experimental investigations on the various aspects of ADS reactors. The MYRRHA - Accelerator Driven System (Multipurpose hYbrid Research Reactor for High-tech Applications) is the world's first large scale Accelerator Driven System project at power levels scalable to industrial systems. The conceptual design of the MYRRHA project began in 2012 and will be operational by 2025. In this project considered a proton beam of 600 MeV with a current of 4 mA impinging on a lead–bismuth spallation target, and ensures a thermal power of 65–100 MWth for subcritical or critical modes (Popescu, 2014). Glinatsis et al. (2017) have theoretically investigated the conceptual design of an accelerator-driven subcritical system fuelled by the (Th, LEU) cycle. They considered a proton beam of 800 MeV with a current of 1 mA, which ensures a thermal power of about 29 MWth for this core. Their results have indicated that the ADS core with the (Th, PU)Ox fuel cycle has good safety performances (Glinatsis et al., 2017). Gholamzadeh et al. (2016) have discussed the neutronic and thermo-hydraulic performances of a modelled accelerator-driven aqueous homogeneous reactor. They considered a 30 MeV proton beam with a 150 μA current.

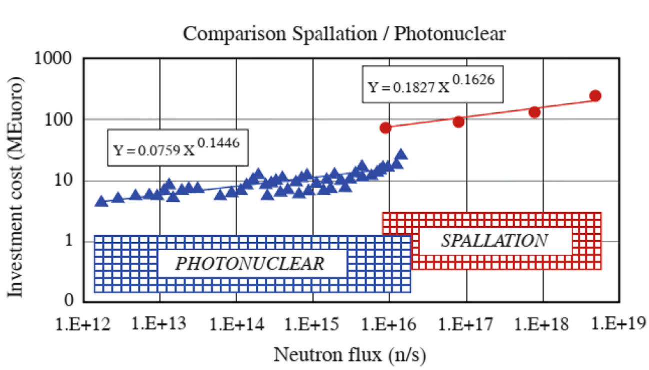

Fig. 1. Spallation versus photonuclear process for neutron production (Feizi and Ranjbar, 2015).

Their calculation showed that the modelled system could be used to produce 4.683 kW fission-related power and an adequate production yield of different radioisotopes per week (Gholamzadeh et al., 2016). The CiADS (China initiative Accelerator Driven System) approved by chinese government at 2016 aims to build the first ADS experimental facility to demonstrate the nuclear waste transmutation. The CiADS driving linac can accelerate 5 mA proton beam to 500 MeV at the beam power up to 2.5 MW (Wang, et al., 2019).

Recently, the use of electron accelerators was noticed because they are inherently compact, economical, reliable, easy to handle, less hazardous and most suitable for applications such as small portable reactor studies (Petwal et al., 2007; Ragab et al., 2019).

Different studies have reported on electron LINAC-based subcritical reactors. Carta et al. (2006) have performed studies on the ENEA RC1, Casaccia TRIGA subcritical reactor. They applied a 25 MeV electron beam with 1 mA electron current and the 1 cm beam width. Their calculations demonstrated that the simulated core made the effective multiplication factor (k_{eff}) less than 0.98. This subcritical core created a power of less than 50 kW for different photoneutron configurations and materials (Carta et al., 2006). Torabi et al. (2013) have reported the theoretical calculations of photoneutron production by a 25 MeV electron linac. They discussed the possibility of using an optimized neutron beam in BNCT (Torabi et al., 2013). O'Kelly (2008) has investigated the TRIGA Mark II research reactor. The TRIGA core linked with a 20 MeV electron accelerator, which the beam current was equal to 80–100 mA. This study of a full-scale ADS system was conducted with a power of several kilowatts at the University of Texas at Austin (UT) (O'Kelly, 2008).

Some previous studies of other researchers have focused on electron accelerator-based subcritical reactors to generate the optimal neutron flux in medical and industrial applications with low thermal power (on the scale of several kilowatts). This research purpose and relevant future studies are the feasibility study into the subcriticalization of the Holos core so that this subcritical core can supply electricity to several houses in remote areas (on the scale of several megawatts). An electron accelerator is used as an external neutron source. Hence, the neutronic performance of the modelled core is discussed to produce the maximum fission rate inside the Holos subcritical core and the cost-effective output power. The solutions have been proposed to improve the neutron performance of the Holos subcritical core.

2. Material and method

The Holos critical nuclear reactor is a distributable modular reactor with enhanced safety features. The specialized configurations of Holos Quad and Titan cores can be airlifted and timely deployed to supply emergency electricity and process heat to disaster areas and inaccessible remote positions (Filippone & Jordan, 2017). In this study, the MCNPX2.6 code is used for calculations and simulations, which is a general-purpose Monte Carlo *N*-Particle code to track 35 types of particles e.g. neutrons, photons, electrons over a broad range of energies (Pelowitz, 2008).

In the critical and subcritical states of Holos core, the four-part cylindrical core has been simulated with 232 Graphite Hexagons and using the MCNPX2.6 code. A hexagonal Graphite block has 19 uranium oxide fuel rods and 54 helium coolant channels with the mentioned dimensions in Table 1. The moderator of the simulated core is the Graphite (Fig. 2). A 3D neutronic model of the Holos core was simulated using MCNPX2.6 code through ENDF/B-VI continuous-energy cross-section. The cross-sections of S(α,β) have been used for the BeO reflector and Graphite moderator. KCODE has been used with 30,000 neutron source histories per cycle, 50 ineffective cycles and 250 effective cycles to calculate neutronic parameters.

The given dimensions of the Holos cylindrical core is equal to height 250 cm and radius 95 cm, and 7.8 % enriched-uranium oxide was selected to achieve an effective multiplication factor (k_{eff}) less than 0.98

Table 1
Overview of Holos critical core properties (Filippone & Jordan, 2017).

Holos critical core properties	Unit	Value
Operating Power	MW_{th}	22
Operating Lifetime (FEPY)	y	10–20
Enrichment Range	%	8–15
Holos fuel cartridge height	cm	250
Holos fuel cartridge radius	cm	95
The number of assemblies in each of the four core sections		58
Fuel Channels in any assembly		19
Fuel Channel Diameter	cm	1.4
Coolant Channels in any assembly		54
Coolant Channel Diameter	cm	0.7
Reflector/ Moderator/ Coolant		BeO/ Graphite/ Helium

(the critical state with 8.6 % enriched-uranium oxide). Fig. 2 demonstrates the simulated model of the Holos core with the MCNPX2.6 code.

The Pb photoneutron target is placed at the centre of the Holos subcritical core to produce primary neutrons (Fig. 3). A 100 MeV-electron beam was considered with a 1 mA current and a beam width of 1 cm. An accelerated electron beam intensely hits a photoneutron target; as a result, (e,γ) and (γ,n) reactions occur within the target. The surrounding subcritical core multiplies leaked photoneutrons from the target. The number of photoneutrons per incident electron depends on the incident electron energy and the atomic number of target.

The deposited power and the flux were calculated inside the simulated core using the mesh tally of the MCNPX2.6 code. Reactivity coefficients of fuel, coolant, and moderator were calculated using the TMP card. The temperature of a cell at the input file is denoted by kT in the unit of MeV. A cell temperature should be written on MeV at the end of the input line related to this cell and simultaneously the related library should be used in the material card, which identifies the cell material. The void reactivity effect of the coolant was calculated for the subcritical core. The delayed neutron fraction and the effective delayed neutron fraction were calculated separately for the Holos core in critical and subcritical levels by the MCNPX2.6 code.

3. Result and discussion

To examine the behaviour of the electron accelerator driven Holos subcritical reactor, the photoneutron target and the energy of the incident electron beam were optimized. The physical and the thermodynamic properties were compared for the selected heavy elements such as Tungsten, Tantalum, Lead, Mercury and Lead (44.5 %)- Bismuth (55.5 %). Their neutronic properties were evaluated for the electron beam with different energies. The results showed that the Lead has the lowest neutron absorption rate and the deposited heat. In the cylindrical optimized target with a 5 cm radius and 6 cm height, the deposited power density inside the target doesn't exceed a few kilowatts because of the high neutron and photon leakage rates. Results showed that the optimized Lead target produced the maximum number of the leakage neutrons for the electron energy range 100 MeV to 1 GeV (the optimal electron energy range). Therefore, the electrons in this energy range have the same neutron value, but the production of high-energy electrons is expensive. According to calculations, the 100 MeV electron beam is favourable for the optimal cylindrical target.

3.1. Effective multiplication factor (k_{eff})

The computational data show, that the effective multiplication factor (k_{eff}) is 0.97352 ± 0.00037 for the Holos modelled subcritical core with the 7.8 % enriched uranium oxide fuel. The uranium oxide enrichment was reduced for the subcriticalitization of the Holos core. Fig. 4 shows the dependence of the total fission power and reactivity (**ρ**) (vertical left scale) and the UO_2 fuel enrichment (vertical right scale) versus the effective multiplication factor (k_{eff}) for the Holos subcritical core.

The efficient sidelong factors in the k_{eff} value variation up to 3000 pcm consist of fuel and coolant temperature enhancement, coolant density reduction and making bubble inside coolant, and so on. Hence, the effective multiplication factor of the Holos subcritical core should be less than 3000 pcm. The Holos subcritical core was adjusted with UO_2 fuel and 7.8 % enrichment so that the effective multiplication factor (k_{eff}) was equal to 0.97.

3.2. Total thermal power

In fuel cells, the released heat of the (n, fission) reaction and the deposited heat rate of all photon reactions (fission and non– fission) are calculated by F7: n and F6: p tallies of the MCNPX 2.6 code separately. Only 96.45 % of the F6:p tally value is the share of the photon fission heat inside the fuel cells. For 1 mA electron beam, the power of the (γ, fission) and (n, fission) reactions of the UO_2 fuel and the total fission power are plotted separately in Fig. 5.

The total thermal power of the Holos subcritical core will be equal to 12 kW for 20 MeV electron energy and 70 kW for 100 MeV electron energy (the accelerator current of 1 mA). By increasing the accelerator current to 100 mA, the subcritical core power will reach 1 MW for 20 MeV electron energy and 7 MW for 100 MeV electron energy.

3.3. Neutronics calculations

There are some neutronic parameters to help the dynamic behaviour investigation of the modelled core. They are used to study the feasibility of the subcriticalization of the Holos simulated core and its optimization (Table 2).

In an accelerator driven, subcritical fission device, the 'primary' (or 'source') neutrons produced via spallation by the interaction of the proton beam with a suitable target, initiate a cascade process. The N_s parameter is equal to the primary photoneutrons. Fission and (n, xn) reactions multiply the source photoneutrons inside the subcritical core through a factor M defined as follows (International Atomic Energy Agency, 2015):

$$M = 1 + k + k^2 + k^3 + \cdots + k^n = \frac{1}{1-k}(pern \rightarrow \infty .and.k < 1) \tag{3-1}$$

The $N_s \times M$ value specifies the total number of generated neutrons after multiplication inside the subcritical core with the multiplication factor (M). In an ADS, the source factor (k_s) is conceptually and numerically different from the effective criticality factor (k_{eff}) due to the presence of an external neutron source. The source factor is related to the location of the external source and its energy, and the effective multiplication factor (k_{eff}) is only relevant to the fundamental mode of the neutron flux distribution inside the reactor core and is independent of the source. The source factor (k_s) of 0.624 is calculated for the Pb photoneutron target in the centre of the Holos subcritical core by MCNPX2.6 code (for 100 MeV electron energy).

The importance of source neutrons (φ^*) defined, (Glinatsis et al., 2017), by the ratio:

$$\varphi^* = \frac{(1-k_{eff})/k_{eff}}{(1-k_s)/k_s} \tag{3-2}$$

In general, φ^* compares the neutrons from the external source (N_{ext}) to those coming from the fission (N_{fiss}). If φ^* less than one, the N_{ext} multiplies less than N_{fiss}. If $\varphi^* = 1$, the external source neutron is equal to the fission one (same energetics and spatial distribution). If φ^* is more than one, the external source brings neutrons from which multiplication is, on average, better than the one obtained by neutrons from fission, and it is the favourable case to optimize the system (International Atomic Energy Agency, 2015).

The calculations showed that the source importance (φ^*) of the Holos subcritical core is equal to 0.045. The energy and spatial distributions of

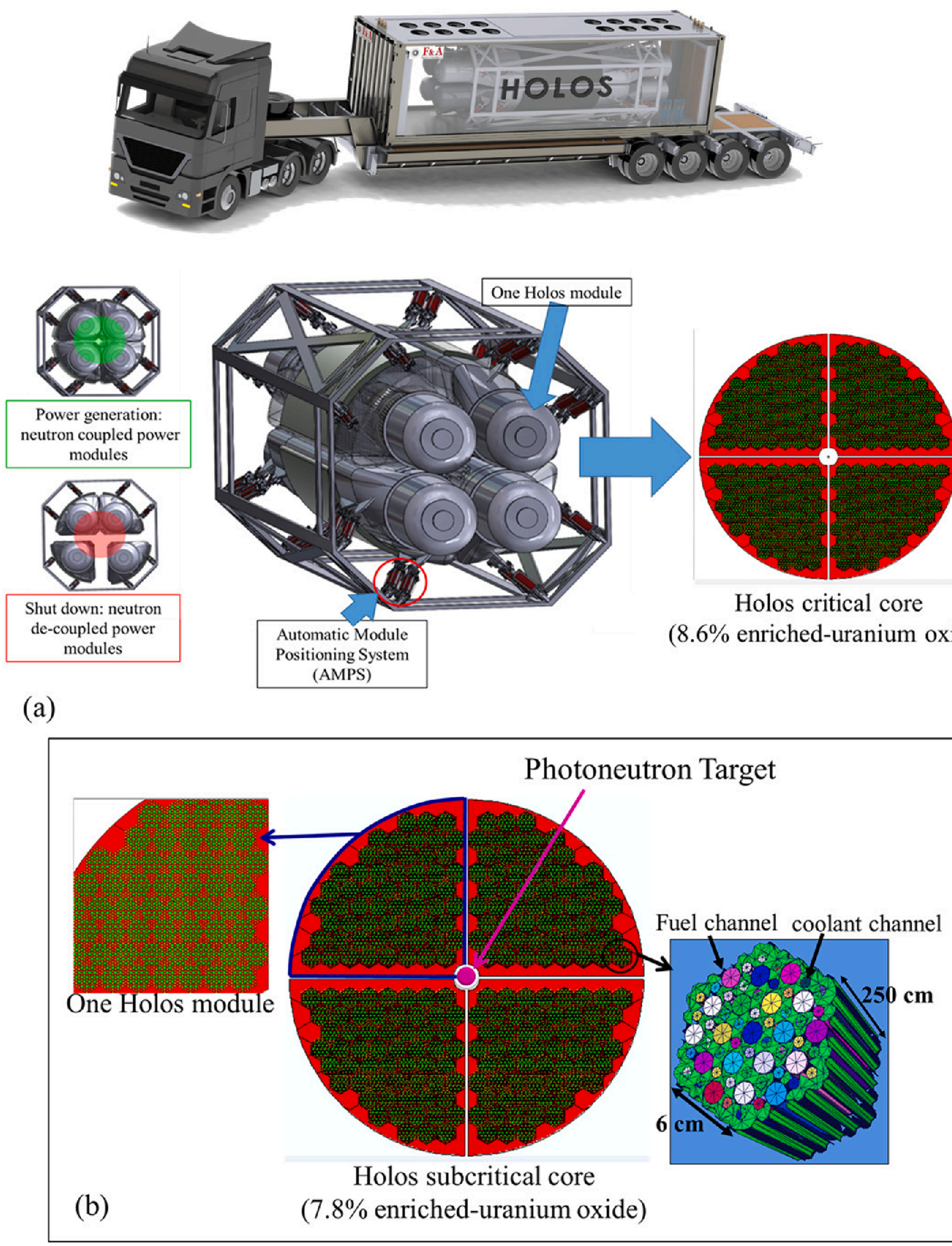

Fig. 2. View of a) Holos core components (critical), b) The computational model of Holos core with uranium oxide by MCNPX2.6 code (subcritical).

the fission neutrons are more dominant than the external source neutrons inside the simulated core. Hence, the multiplication of fission neutrons occurs better than the external source neutrons. The photoneutron source can confine, and it should avoid wasting photoneutrons as much as possible to increase the source importance factor (φ^*). If the ratio of the photoneutron diffusion length to the size of the fissile core increase, the possibility of (n, nx) and (n, fission) reactions grows. As a result, the importance of external source photoneutrons increases.

It can be investigated the spatial distribution of external source photoneutrons entering the modelled core, and the content of the fuel rods can be changed so that they are most likely to be exposed to these photoneutrons. Therefore, the source photoneutrons will produce more multiplication reactions within the subcritical core. The distribution of several photoneutron targets can examine inside the subcritical core. The energy spectrum of these photoneutrons must be modified to be compatible with the energy of fission-generating neutrons within the fissile core. In these cases, photoneutrons would produce more multiplication reactions inside the modelled core. The coefficient of "f "will decrease by using these efficient factors at the enhancement of the source importance factor (φ^*).

The critical reactors operate at any power that can safely remove, but the power level of an ADS reactor is related to the accelerator current (i). The generated power of the ADS reactor can write as follows (International Atomic Energy Agency, 2015):

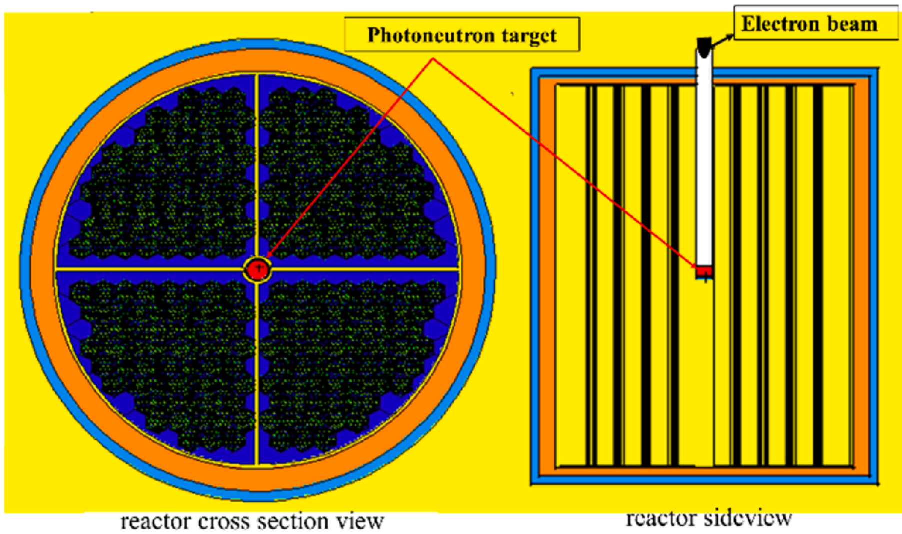

Fig. 3. Simulated view of photoneutron target inside the Holos subcritical reactor by MCNPX2.6 code.

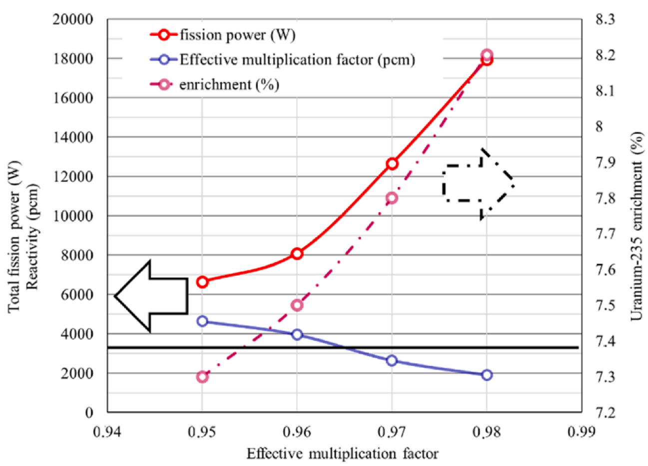

Fig. 4. The total fission power and reactivity (**ρ**) (vertical left scale) and the Holos subcritical core enrichment (vertical right scale) vs the effective multiplication factor (k_{eff}).

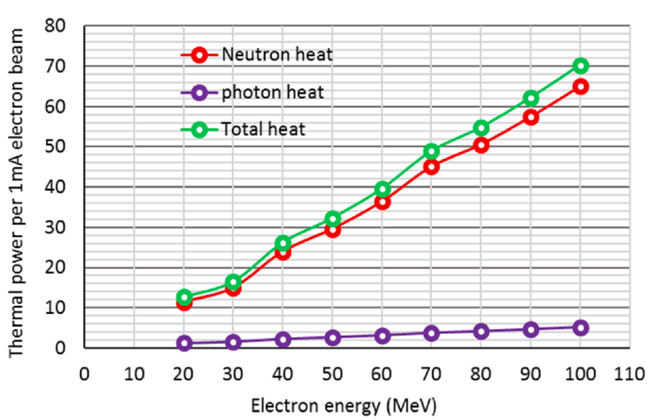

Fig. 5. The power of the (γ, fission) and (n, fission) reactions of the UO_2 fuel and the total fission power vs different electron energies.

Table 2
Neutronic and dynamic parameters of a 1 mA electron accelerator-based subcritical reactor.

Factor	Value
Source multiplication factor (M)	2.6596
External source yield factor (Z)	4.98
Accelerator Power (P_{Acc} (MW))	0.1
Source importance (φ^*)	0.045

$$P_{tot} = \left(\frac{k_{eff}}{1-k_{eff}}\right).\left(\frac{P_{Acc}.Z.\varphi^*}{E_e}\right).\left(\frac{\overline{E}_f}{\upsilon}\right)\mathrm{P_{tot}} = \left(\frac{\mathrm{K_{eff}}}{1-\mathrm{K_{eff}}}\right).\left(\frac{\mathrm{P_{Acc}}.Z.\varphi^*}{\mathrm{E_e}}\right).\left(\frac{\overline{\mathrm{E}}_f}{\upsilon}\right) \tag{3-3}$$

Where Z is the yield of photoneutrons for an external neutron source, and the parameter υ is the average number of neutrons emitted per fission. The accelerator power is defined as follows (International Atomic Energy Agency, 2015):

$$P_{Acc}(MW) = i_e(mA) \times E_e(GeV) \tag{3-4}$$

Where E_e is the energy of the external electrons. Hence, the ratio between the needed power of the accelerator, and the electric output power of the ADS reactor is equal to “f “ (International Atomic Energy Agency, 2015):

$$f = \frac{P_{acc}}{P_{tot}} = \frac{E_e}{Z\varphi^* E_f}\left(\frac{1-k_{eff}}{k_{eff}}\right)\upsilon f = \frac{\mathrm{P_{acc}}}{\mathrm{P_{el}}} = \frac{\mathrm{E_e}}{Z\varphi^*\mathrm{E_f}}\left(\frac{1-\mathrm{k_{eff}}}{\mathrm{k_{eff}}}\right)\upsilon \tag{3-5}$$

If the coefficient of “f” is more than one, the accelerator consumes more energy than what the reactor can provide. If the “f” coefficient is less than one, the subcritical system produces more energy than the accelerator consumption. The calculations show that the “f” coefficient of the modelled subcritical system is equal to 0.1887, and as a result, this system produces more energy than the accelerator consumption. The Holos subcritical system can supply both the accelerator consumption power and the electricity demand of a region. As the number of source photoneutrons increases, the value of the “f” coefficient decreases, and it is a favourable state. A proposed solution of the photoneutron enhancement is the usage of multiple neutron targets inside the subcritical core, and so the production power capacity of the subcritical reactor also improves.

Some safety parameters were calculated, such as the effective fraction of delayed neutrons (**β_{eff}**), the fraction of delayed neutrons (**β**), temperature reactivity coefficients of the fuel (**($\Delta\rho/\Delta T)_{fuel}$**), coolant (**($\Delta\rho/\Delta T)_{reflector}$**) and moderator (**($\Delta\rho/\Delta T)_{moderator}$**).

Table 3 shows the safety parameters of the Holos core in subcritical and critical levels by the MCNPX2.6 code. In the Holos subcritical core, the results show that the temperature reactivity coefficient of the Helium coolant and the BeO reflector is a small positive value. This parameter is well negative in the case of the UO_2 fuel and the Graphite moderator.

The effective fraction of delayed neutrons (**β_{eff}**) reflects the ability of the reactor to thermalize and utilize each neutron produced. The **β** is not the same as the **β_{eff}** due to the fact delayed neutrons do not have the same properties as prompt neutrons released directly from fission. In general, delayed neutrons have an average energy of 0.4 MeV, which is lower than the average energy of 2 MeV for prompt neutrons. In the Holos subcritical core, the results show that the **β_{eff}** and **β** fractions are more than one in the Holos critical core (Table 3).

The void reactivity coefficient is another one of the safety parameters, which is calculated for the Holos modelled reactor. In the Holos subcritical reactor, the coolant is helium gas. As the temperature of the reactor core increases, the density of the liquid or gas components of the core decreases. As a result, voids are created inside the coolant, and the reactivity of the subcritical core changes.

The relation of $\rho = \rho_0$ (1-void%) shows the effect of the reactor temperature increase on the coolant density. The new density (ρ) of the coolant obtains for each of the void percentages (10 % to 90 %). The new reactivity of the Holos subcritical core was calculated for each change step of the coolant density via MCNPX2.6 code.

Fig. 6 displays the trend of reactivity variations versus different void percentages. The calculations demonstrate that the void reactivity coefficient of the Helium coolant is positive for the Holos critical core, and it slowly decreases as the void percentage increases. This coefficient is negative for the Holos subcritical core considerably and increases more rapidly than the critical state as the void percentage increases.

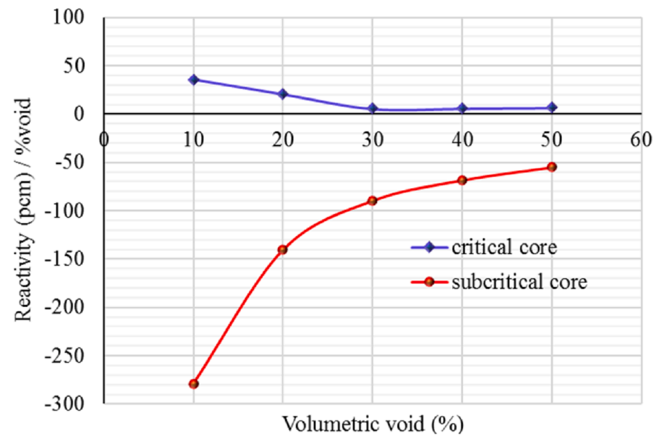

Fig. 6. The ratio of reactivity (ρ) to %void in the critical and the subcritical levels.

3.4. Deposited power density

The results show that total power density of 36.5 kW/cm^3 was deposited inside the Pb photoneutron target. The external photoneutron source with 100 MeV electrons and 1 mA current was considered to induce the Holos subcritical core. Fig. 7 shows our calculated results for the distribution of the neutron deposited power at the axial and radial directions for the subcritical and critical states. The calculations show that central parts of the subcritical core and its indoor edges have the highest deposited power (the maximum power density of 20 mW/cm^3). In general, the neutron deposited power of the subcritical core is less than the critical core (the maximum power density of 18 mW/cm^3), and the Holos critical core has a smooth power distribution of neutrons at the radial and axial directions. Due to the source photoneutron distribution inward the Holos subcritical core, many hot points were created inside the core. For the most central fuel rod of the Holos subcritical core, the deposited power (13.5 kW/cm^3) is twice the deposited power inside the most central rod of the Holos critical core (6.1 kW/cm^3). In done calculations of this designed Holos core with 7 MW-output power, a 100 mA-electron accelerator is used. (Reviewer#1 s' comment).

Fig. 8 displays the distribution of the photon deposited power at the axial and radial directions for the subcritical and critical levels. The calculations show that more photon power is deposited at the central part of the subcritical core (the maximum power density of 7 mW/cm^3), while the smooth power distribution of photons is observed throughout the critical core (the maximum power density of 0.97 mW/cm^3). The power density of the Holos critical core is 3.46 W/cm^3, and one is 0.99 W/cm^3 in the Holos subcritical core.

Holos generators adopt a unique architecture that integrates proven commercial technologies to produce affordable pollutant-free electricity with safer melt-tolerant fuels. In the Holos configuration, to further increase safety, the air (used in the conventional turbojet system) was replaced with the Helium gas whose energy content is increased as it flows through the fuel cartridge to expand through turbo-machinery and produce electricity (Filippone & Jordan, 2017). This unique turbojet system causes to flow the deposited heat in the Holos core centre towards the electricity generator. Therefore, the turbojet system prevents depositing a large heat inside the photoneutron target and the core centre (Fig. 9).

3.5. Flux distribution

In this work was calculated the neutron flux distribution at the axial and radial directions of the Holos core for critical and subcritical states (Fig. 10).

The calculations demonstrate that the central parts of the Holos radial direction receive the highest neutron flux in the critical and subcritical levels. According to the results, the radial distribution of the neutron flux within the subcritical core is greater than the critical core, and the neutron flux distribution of the Holos subcritical core changes with a steep slope.

Fig. 11 shows the results of the photon flux distribution at the axial and radial directions for the Holos critical and subcritical cores. The calculations indicate that the central parts of the Holos radial direction receive the highest photon flux in critical and subcritical states. According to the results, the radial distribution of the photon flux inside the Holos subcritical core is sharper than one inside the Holos critical core.

A prominent feature of subcritical reactors is the high flux distribution of neutrons and photons within the reactor core. This high particle flux can be used to make radioisotopes and convert long-lived isotopes in the hazardous nuclear waste. The maximum neutron flux of $\sim 2 \times 10^{12}$n/s.cm^2 produced in the Holos subcritical core is suitable to be applied for different research purpoces. This range of the neutron flux will be helpful to use long-lived actinides or the fertile and fissile

Table 3
Safety parameters of the Holos core calculated in subcritical and critical levels by MCNPX 2.6.0.

	β (pcm)	β_{eff} (pcm)	$(\Delta\rho/\Delta T)_{fuel}$ (pcm/K)	$(\Delta\rho/\Delta T)_{moderator}$ (pcm/K)	$(\Delta\rho/\Delta T)_{coolant}$ (pcm/K)	$(\Delta\rho/\Delta T)_{reflector}$ (pcm/K)
Critical	657	738	−6.1228	−0.2787	−0.18354	−0.1835
Subcritical	815	816	−6.3612	−0.0609	0.03655	0.0365

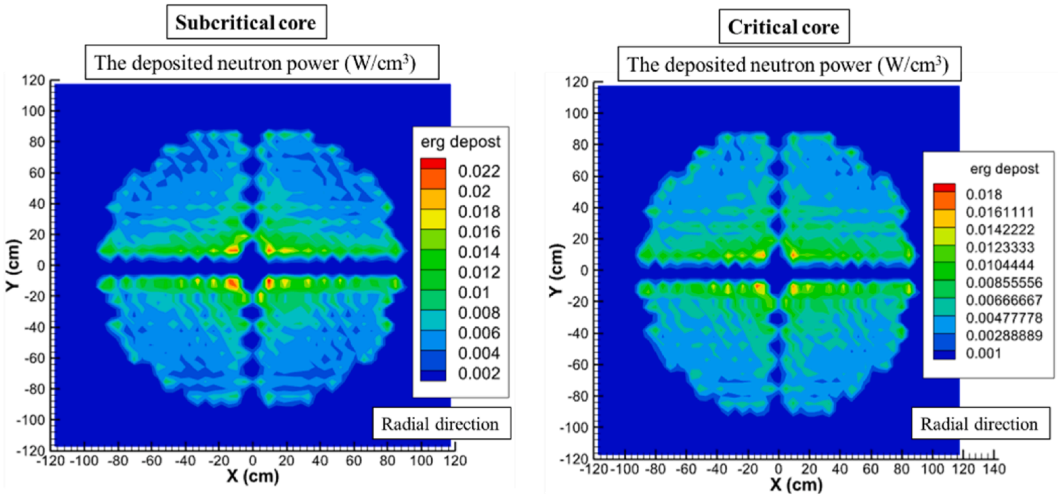

Fig. 7. Radial distribution of deposited neutron power inside the Holos core in the subcritical and critical states, calculated in this work.

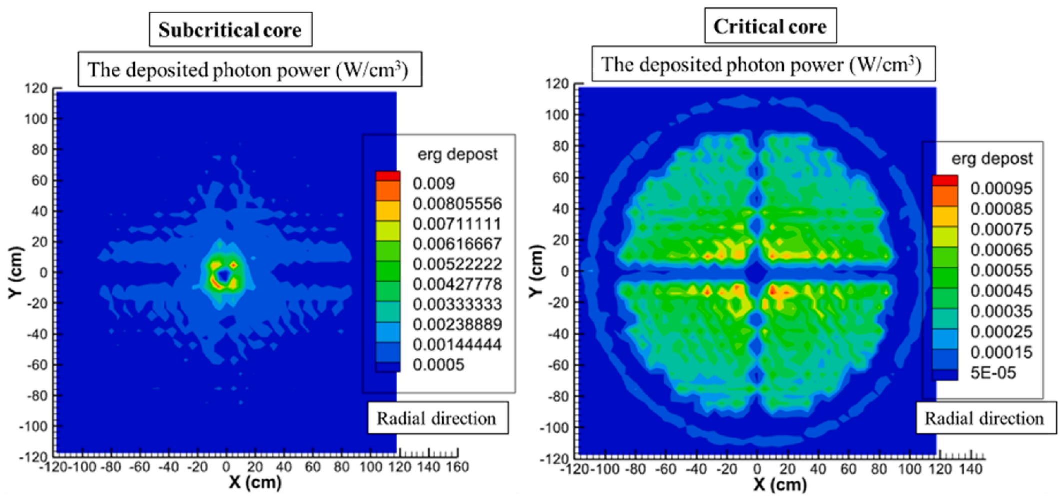

Fig. 8. Radial distribution of deposited photon power inside the Holos core in the subcritical and critical states, calculated in this work.

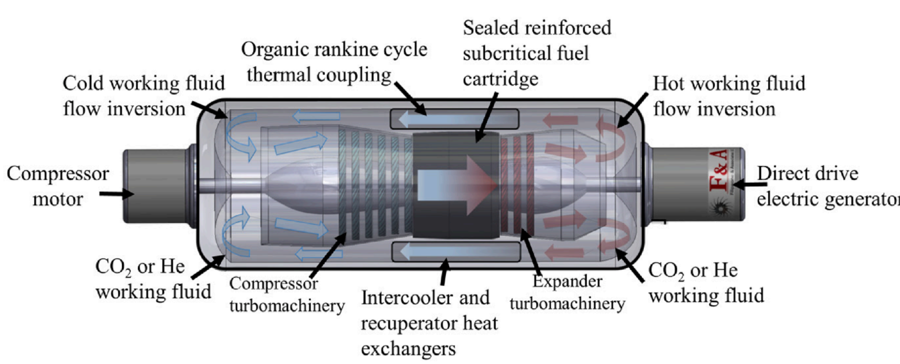

Fig. 9. a “closed-loop” turbojet engine with Holos sealed fuel cartridges.

isotopes as the subcritical reactor fuel.

4. Conclusion

The Holos subcritical reactor is more reliable and safer than a critical small reactor. This type of the portable reactor can use to supply electricity in remote areas and emergencies. The High flux distributions of particles and the negative reactivity coefficients are advantages of the Holos subcritical core. In addition, the design of SMR and ADS reactors can be considered because of other advantages such as higher burn-up, independence to control rods and operating in the subcritical level. The neutronic investigation of the Holos subcritical core shows that they can desirably produce domestic electricity supply at safe and economic conditions. The Holos subcritical core can produce a total thermal power

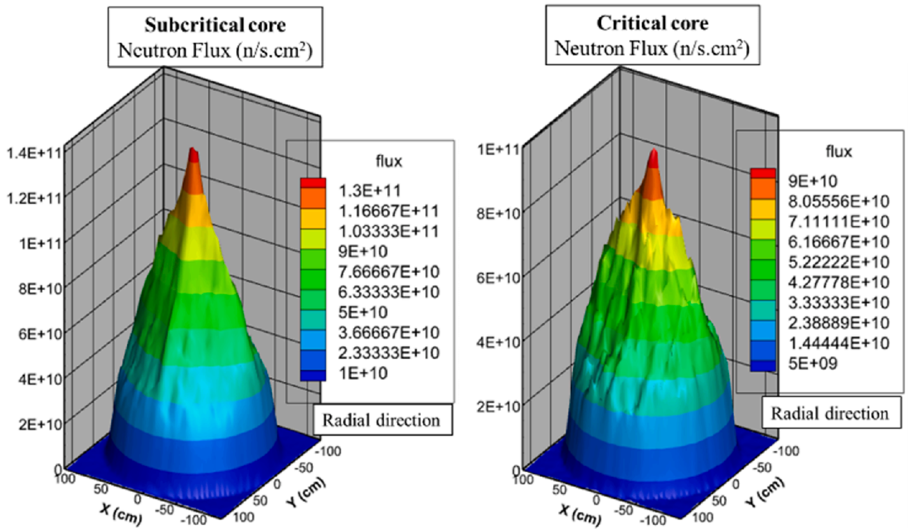

Fig. 10. Radial distribution of neutron flux inside the Holos core in the subcritical and critical states, calculated in this work.

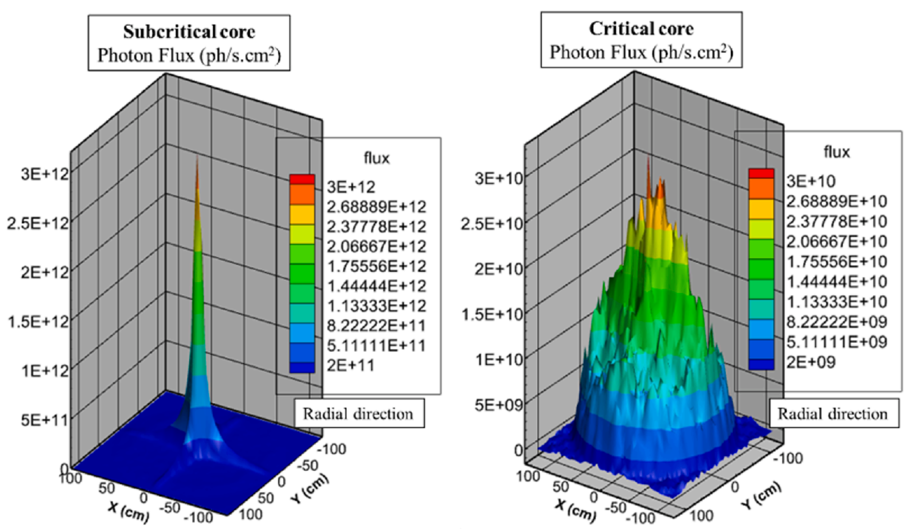

Fig. 11. Radial distribution of photon flux inside the Holos core in the subcritical and critical states, calculated in this work.

of 7 MW that driven by a 100 MeV electron accelerator with a 100 mA current. The calculations demonstrate that the "f"coefficient of the modelled subcritical system is equal to 0.1887, and this Holos system produces more energy than the accelerator consumption. In general, the Holos critical core has a smooth power distribution at the radial and axial directions, and the neutron flux distribution within the critical core is less than that inside the Holos subcritical core. The turbojet cooling system causes to flow the deposited heat in the Holos core centre towards the electricity generator, and the high heat does not deposit in the subcritical core centre. The Holos subcritical core can be improved to yield a smoother and higher production rate of particles with the design of other external sources inside the core. Burnup calculations of the Holos core will be examined with the MCNPX2.6 code. The neutronic behaviour of the Holos subcritical core can discuss with other fissile and fertile fuels.

CRediT authorship contribution statement

Mohammad Mahdi Firoozabadi: Conceptualization, Methodology, Writing – review & editing, Supervision. **Sareh Arhami:** Conceptualization, Methodology, Software, Validation, Formal analysis, Investigation, Data curation, Writing – original draft, Writing – review & editing, Visualization. **Zohreh Golamzadeh:** Conceptualization, Methodology, Software, Data curation, Project administration. **Mahdi Zangian:** Methodology.

Declaration of Competing Interest

The authors declare that they have no known competing financial interests or personal relationships that could have appeared to influence the work reported in this paper.

Acknowledgments

The authors are grateful to Birjand University and Reactor Research School, Nuclear Science and Technology Research Institute for supporting the research.

References

Carta, M., Burgio, N., D'Angelo, A., Santagata, A., Petrovich, C., Schikorr, M., . . . Salvatores, M. (2006). Electron versus proton accelerator driven sub-critical system performance using TRIGA reactors at power. *43129862. 43*. United States: American

Nuclear Society - ANS. Retrieved from http://inis.iaea.org/search/search.aspx?orig_q=RN:43129862.

Filippone, C., Jordan, K. (2017). The Holos Reactor: A Distributable Power Generator with Transportable Subcritical Power Modules. *8708 48th Place, College Park MD 20740*. doi:10.31224/osf.io/jzac9.

Feizi, H., Ranjbar, A.H., 2015. Design and parameter optimization of a small-scale electron-based ADS for radioactive waste transmutation. Eur. Phys. J. Plus 130 (5), 99. https://doi.org/10.1140/epjp/i2015-15099-y.

Gholamzadeh, Z., Mirvakili, S.M., Davari, A., 2016. Neutronic and thermo hydraulic analysis of a modeled subcritical uranyl nitrate aqueous reactor driven by 30-MeV protons. Ann. Nucl. Energy 171–178. https://doi.org/10.1016/janucene201606037.

Glinatsis, G., Carta, M., Gugiu, D., 2017. Conceptual design of a sub-critical Pb-cooled Accelerator Driven System (ADS) fuelled by (Th-LEU). Ann. Nucl. Energy 104, 1–8. https://doi.org/10.1016/j.anucene.2017.02.005.

Ingersoll, D.T., Houghton, Z.J., Bromm, R., Desportes, C., 2014. NuScale small modular reactor for Co-generation of electricity and water. Desalination 340, 84–93. https://doi.org/10.1016/j.desal.2014.02.023.

International Atomic Energy Agency, 2015. Status of Accelerator Driven Systems Research and Technology Development, TECDOC Series. Retrieved from. https://www.iaea.org/publications/10870/status-of-accelerator-driven-systems-research-and-technology-development.

Magruder, S., Jackson, D., Thomas, K., Herviou, K., Dupuy, P., Devos, M., Cook, S. (2018). *SMR Regulators' Forum pilot project report Considering the application of a graded approach, defence-in-depth and emergency planning zone size for Small Modular Reactors.* International Atomic Energy Agency (IAEA): IAEA. Retrieved from http://inis.iaea.org/search/search.aspx?orig_q=RN:51001163.

Nifenecker, H., David, S., Loiseaux, J., Meplan, O., 2001. Basics of accelerator driven subcritical reactors. Nucl. Instrum. Methods. Phys. Res. B Nucl. Instrum. Meth. A 463 (3), 428–467. https://doi.org/10.1016/S0168-9002(01)00160-7.

O'Kelly, D.S., 2008. Operation and Reactivity Measurements of an Accelerator Driven Subcritical TRIGA Reactor. The University of Texas, Austin.

Pelowitz, D.B. (2008). MCNPX User's Manual. Version 2.6.0.s.l. *Los Alamos National Laboratory (LANL), LA-CP-07-1473.*

Petwal, V.C., Senecha, V.K., Subbaiah, K.V., Soni, H.C., Kotaiah, S., 2007. Optimization studies of photo-neutron production in high-Z metallic targets using high energy electron beam for ADS and transmutation. Pramana 68 (2), 235–241. https://doi.org/10.1007/s12043-007-0027-3.

Popescu, L., 2014. Nuclear-physics applications of MYRRHA. EPJ Web Conf. 66, 10011.

Ragab, F.M., Elsaady, E., Abuzeid, H., Nada, A., ElAshmawy, M., 2019. Characterization of photo-neutrons produced by 150 MeV and 1 GeV electrons impinging on high Z-metallic targets for neutron resonance spectroscopy. Arab J. Nucl. Sci. Appl. 52 (2), 162–168. https://doi.org/10.21608/ajnsa.2019.3755.1088.

Torabi, F., Masoudi, S.F., Rahmani, F., 2013. Photoneutron production by a 25 MeV electron linac for BNCT application. Ann. Nucl. Energy 54, 192. https://doi.org/10.1016/j.anucene.2012.11.001.

Wang, Z., Wang, F., Huang, G., Wan, Y., Yue, W., Liu, S., He, Y., 2019. The status of CiADS superconducting LINAC. 10th International Particle Accelerator Conference.